Numerical study on long-term monopile foundation response

Song-Hun Chong & Cesar Pasten

Taylor & Francis
Taylor & Francis Group

Numerical study on long-term monopile foundation response

Song-Hun Chong[a] and Cesar Pasten[b]

[a]Metropolitan Transportation Systems Research Center, Korea Railroad Research Institute, Gyeonggi-do, South Korea; [b]Department of Civil Engineering, University of Chile, Santiago, Chile

ABSTRACT

This paper analyzes the long-term monopile foundation that undergoes numerous mechanical cycles. The semiempirical scheme is adopted to involve a mechanical constitutive model to extract stress and strains at the first cycle and polynomial-type strain accumulation functions to track the progressive plastic deformation. In particular, the strain function contains the fundamental features that require simulating the long-term response of geomaterials: volumetric strain (terminal void ratio) and shear strain (shakedown or ratcheting), the strain accumulation rate, and stress obliquity. The numerical simulation shows evolution of displacements, pile rotation, and stress redistribution along the embedded pile as the number of load cycles increases. The analysis highlights that the pile rigidity affects the pattern of horizontal stress and displacement. The repetitive lateral load enhances the lateral load resistance due to soil densification along the pile.

Introduction

Renewed attention is rapidly driven by the long-term pile foundation for offshore wind turbines to benefit from the use of wind as renewable energy. The selection of offshore foundation mainly depends on water depth, sediment properties, loading types, and available construction method. Among offshore foundations such as gravity base, suction caisson, and tripod, a monopile has been the most commonly selected foundation type due to its lower cost, simple construction, and appropriateness for shallow water (AWS Truewind 2009; Malhotra 2010). Soils around monopile foundation subjected to numerous mechanical loading experience progressive accumulation of plastic deformation. The progressive displacement that occurs during long-term operation of wind turbine can inflict serious damage to the offshore foundation performance. (Niemunis, Wichtmann, and Triantafyllidis 2005; Achmus, Kuo, and Abdel-Rahman 2009). Thus, the numerical simulation of monopile foundation can help to evaluate and predict the surrounding soil response during large number of cycles.

This study focuses on analyzing the long-term response of monopile foundation. The numerical approach follows the semiempirical explicit scheme that combines modified Cam-Clay (MCC) model to extract the stress and strains at the end of the first cycle and empirical strain accumulation functions to track the progressive plastic deformation. In particular, the polynomial-type function is implemented to save the computational cost by avoiding the cumbersome process at every incremental cycle and contains the fundamental features of long-term soil response that require simulating the long-term response of geomaterials: volumetric strain (terminal void ratio) and shear strain (shakedown and ratcheting), the strain accumulation rate, and stress obliquity. This paper begins with

a review of long-term numerical modeling scheme, followed by a model calibration and monopile foundation simulation.

Numerical modeling of boundary value problems

Numerical scheme

Classical constitutive models that can cause plastic strain during few cycles (i.e., loading and unloading) fail to yield cumulative plastic strains in every loading cycle. The geostructures subjected to cyclic load can be simulated by tracking each cyclic response. In the implicit calculation of accumulation strains, each cycle is incrementally calculated with complicated constitutive model and produces unclosed loop in the stress–strain response. But, the implicit approach hinders capturing physical deformation response due to larger accumulation of numerical errors compared to incremental strain rate; it is limited to predict the long-term response (Wichtmann, Niemunis, and Triantafyllidis 2005; Achmus, Kuo, and Abdel-Rahman 2009). The strain accumulation can be tracked with empirical approaches that fit experimental results with number of load cycles, yet their use is restricted to boundary value problems that need to satisfy with force equilibrium and strain compatibility. Semiempirical scheme that the current step is calculated with values from the previous converged step has been used by incorporating classical constitutive model into empirical accumulation functions to overcome those limitations (Suiker and de Borst 2003; Niemunis, Wichtmann, and Triantafyllidis 2005; François et al. 2010; Kuo, Achmus, and Abdel-Rahman 2012; Pasten, Shin, and Santamarina 2014). Strain accumulation function in explicit calculation is closely related to computational cost. The previously suggested accumulation functions require a numerical cutoff criterion to stop

CONTACT Song-Hun Chong ✉ songhun.chong@gmail.com ⬚ Metropolitan Transportation Systems Research Center, Korea Railroad Research Institute, 176, Cheoldo bangmulgwan-ro, Uiwang-si, Gyeonggi-do 437-757, South Korea.
Color versions of one or more of the figures in the article can be found online at www.tandfonline.com/umgt.

accumulating plastic strain when cyclic strain drops below elastic threshold or when the void ratio reaches the terminal void ratio. For example, accumulated volumetric strain in log-linear-type function is asymptotically incorrect ($\varepsilon_v^{acc} \rightarrow \infty$ as $N \rightarrow \infty$) and the criterion at every incremental cycle should be checked with strains for all nodes. Accordingly, the computational complexity requires higher computation cost during large number of cycles. As an alternative function, the polynomial-type model involved the criterion itself is suggested to (1) save the computational cost by avoiding the cumbersome process at every incremental cycle and (2) contain the fundamental features of long-term soil response that require simulating the long-term response of geomaterials: volumetric strain (terminal void ratio) and shear strain (shakedown and ratcheting), the strain accumulation rate, and stress obliquity. Possible strain accumulation functions are listed in Chong and Santamarina (2016).

Semiempirical explicit scheme used in this study mainly consists of two parts (Figure 1). In the first part (Step 1: stage O–stage C), the geostatic stress and the first cyclic load are applied at the monopile head using MCC model built in ABAQUS 6.14 program; the average horizontal load (H_{avg}) and its amplitude (ΔH) exerted to the pile head are defined by the lateral resistance (H_{ult}) and amplitude ratio. The stress and strain induced by the first loading–unloading cycle are calculated for the initial condition of second part (Step 2–Step 4). The second part is implemented using UMAT subroutine in ABAQUS to track the volumetric and shear strains that accumulate during repetitive loading using polynomial-type empirical accumulation functions. Cumulative strains at $N + \Delta N$ are predicted and imposed for each element, the stress increment is obtained from the accumulated strain vector defined by plasticity, and then numerical iteration is applied until the system can satisfy compatibility and force equilibrium (for more details, refer to Pasten, Shin, and Santamarina 2014).

Table 1. Calibrated model parameters from this study. Initial k_o value is obtained from other parameters of modified Cam-Clay model (details in Muir Wood 1990).

|	Symbol	Value
(a) Modified Cam-Clay parameters		
Unit weight [kN/m³]	γ	18.0
Isotropic compression [·]	λ	0.01
Isotropic recompression [·]	κ	0.001
Drained Poisson's ratio [·]	υ	0.3
MCC strength (for AC)	M	1.42
Void ratio at 1 kPa	$e_{1\,kPa}$	0.955
Coefficient of earth pressure at rest	k_o	0.58
(b) Empirical accumulation functions		
Accumulated strain-rate parameter	α	1.14
Accumulated volumetric strain $\Delta\varepsilon_v^{acc}\big|_N$	a1	1.34
	a2	0.5
Accumulated shear strain $\Delta\varepsilon_q^{acc}\big|_N$	b1	−6.21
	b2	0.0
	c1	0.0

MCC, modified Cam-Clay.

Model calibration

A simple constitutive model is sought for this study, which can capture the stress-dependent soil stiffness and strength and prefailure plastic strain. MCC model built in ABAQUS program is selected herein. The model is calibrated using the published data obtained from the oedometer cell and vertical load cycles. The results show the evolution of void ratio against the event number for different initial packing densities (Chong and Santamarina 2016). The constitutive parameters are defined by formal inversion (Table 1). The stress path associated to cyclic loading under a zero-lateral strain condition is presented in Figure 2. The static loading O follows the ko-compression line. An additional vertical stress increment (i.e., from state O to A) pushes the grains between each other and locks the horizontal movement. As a result, the increased horizontal stress causes a reduction of the deviatoric stress upon vertical stress unloading from state A to B. The
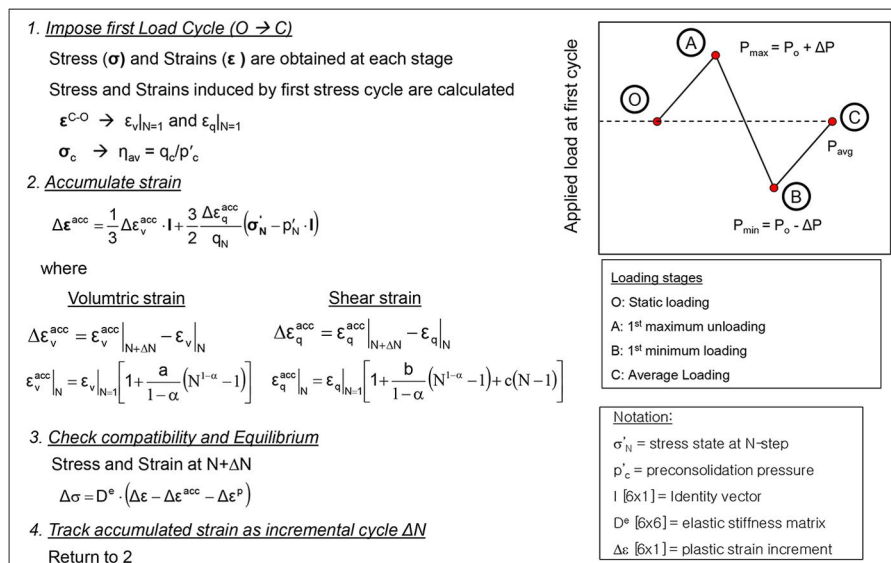

Figure 1. Numerical algorithm that combines a modified Cam-Clay model to extract the stress and strain from the static load (step O) to average load (step C) into polynomial-type strain accumulation function to track deformation response during repetitive loading. The semiempirical explicit scheme is implemented using ABAQUS (step 1) and UMAT subroutine (step 2–step 4).
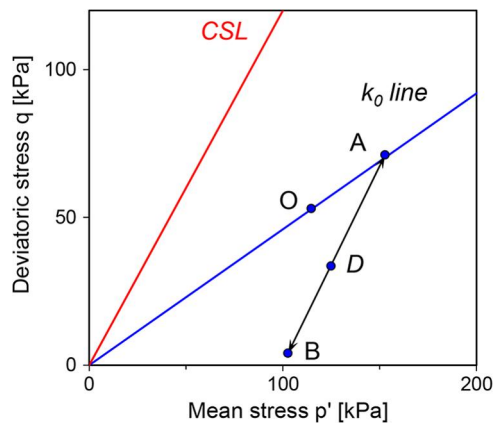
Figure 2. Stress path defined by repetitive loading under zero-lateral strain condition. Note that CSL is critical state line.

"lock-in porosity" that occurs under the repetitive ko-loading produces more plastic strains. Figure 3 shows the comparison between experimental data and numerical simulation for volumetric and deviatoric strain. The model captures experimental results well with the adopted densification rate parameter. In addition, the parameters calibrated under ko-conditions can be tested in triaxial conditions to verify the rate of strain accumulation for different stress obliquity values.
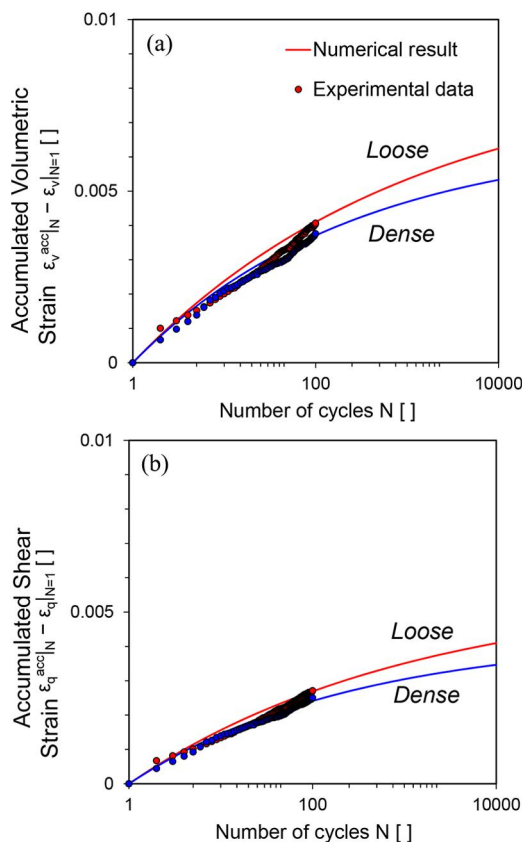
Figure 3. Calibration of the strain accumulation function using repetitive loading test under zero lateral strain condition. (a) accumulated volumetric strain; (b) accumulated shear strain. The average stress obliquity n_{avg} is 0.26. Case is Blasting sand (initial static stress $\sigma'_o = 100$ kPa and vertical cyclic stress amplitude $\Delta\sigma'_v = 100$ kPa). Data from Chong and Santamarina (2016).

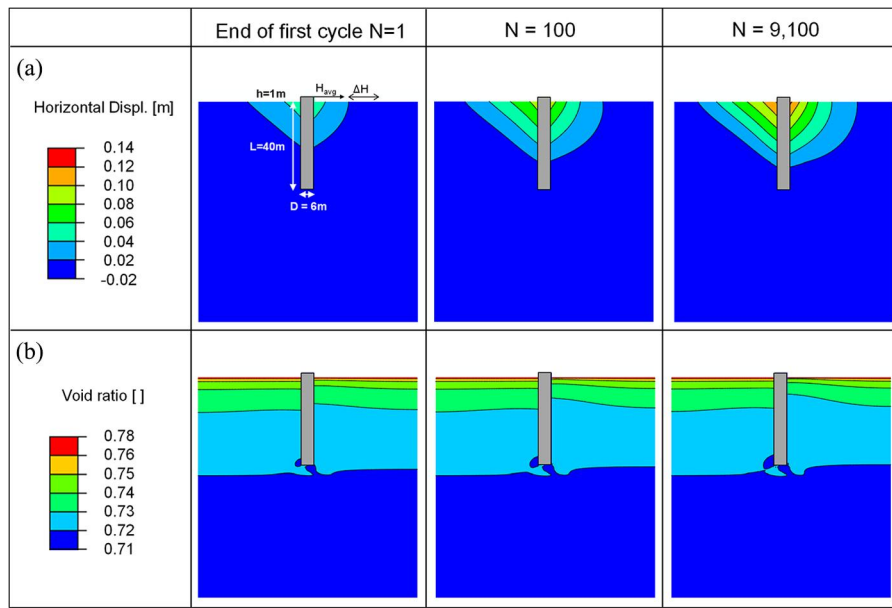## Simulation of monopile foundation

Static load

Finite element software ABAQUS is used to simulate Monopile response, and plane strain boundary condition is applied with four-node full integration elements. Vertical displacement is allowed on side boundaries, the bottom boundary is pinned, and the top surface is free. The lateral boundary effects are investigated for a large number of cycles as worst case. Displacement field (Figure 4a) shows that the far-field surface settlement profile is zero at the end of cycle ($N = 9,100$). Thus, we confirm the proper domain size for the long-term simulation. The pile is modeled as linearly elastic material: pile made of concrete unit weight $\gamma_{con} = 25$ kN/m³, Young's modulus $E_{con} = 200$ GPa, and Poisson's ratio $v_{con} = 0.3$. Contact elements based on coulomb friction theory are used to improve contact interaction between the pile and soil elements. The value of δ/ϕ' varies between 0 and 1, depending on surface roughness, mean particle size of the sand, and the method of installation (Tiwari and Al-Adhadh 2014). As in the case of smooth steel pipe pile, δ ($\sim$23.3°) is taken as two-thirds of the critical friction angle.

Numerically computed load resistance is obtained from formal load control that increases the applied horizontal load on the pile head until numerical instability occurs. Numerically computed load matches well with Zhang's method that assumes the nonlinear-horizontal stress trend along the pile (Zhang, Silva, and Grismala 2005).

Repetitive load

A monopile foundation on sand is simulated by imposing a static load (H_{avg}) followed by repetitive lateral load ($H_{avg} \pm \Delta H$). The numerically predicted lateral resistance is $H_{ult} = 21.5$ MN. The allowable average static load $H_{avg} = 3.6$ MN (FS = 6) and cyclic load amplitude $\Delta H = 0.54$ MN ($0.15 \cdot H_{avg}$) are applied on the node at pile top. Figure 3 presents the redistribution of stress and strain fields with number of cycles. The horizontal repetitive load produces horizontal displacements (Figure 4a). The plastic displacement initiates at soil elements located on the ground surface, yet propagates along the soil elements up to neighboring toe of pile. The repetitive loads produce additional horizontal displacement of 7 cm after $N = 9,100$. Correspondingly, void ratio field shows "soil densification effect" (Figure 4b). The void ratio is gradually decreased at the passive side and the end of pile.

Horizontal load amplitude that plays a crucial role in predicting long-term pile response has pronounced effect on the accumulation of vertical and horizontal displacements (Figure 5). Both displacements increase proportional to the repetitive load amplitude; horizontal displacement is larger than vertical displacement. Most of the displacements occur during early cycles ($N < 100$), yet their accumulation rate is decreased for a large number of cycles. The asymptotic displacement increases with higher horizontal load amplitude. Figure 6 shows the effect of pile geometry on evolution of displacements. The longer and larger pile produces larger displacements. The repetitive lateral load yields an additional horizontal displacement. As anticipated, the cumulative displacements could be

Figure 4. Monopile foundation response to horizontal repetitive load: (a) accumulation of horizontal displacement; distribution of (b) void ratio for load cycles $N = 1$, 100, and 9,100. The average and cyclic loads are $H_{avg} = H_{ult}/6 \sim 3.6$ MN and $\Delta H = 0.15 \cdot H_{avg} \sim 0.54$ MN for an ultimate lateral resistance $H_{ult} \sim 21.5$ MN. Note that the deviatoric stress follows octahedral definition.

more pronounced as the factor of safety decreases. Note that if the same magnitudes of horizontal load are applied to different piles, the longer embedded pile undergoes less displacement and lower accumulation rate.
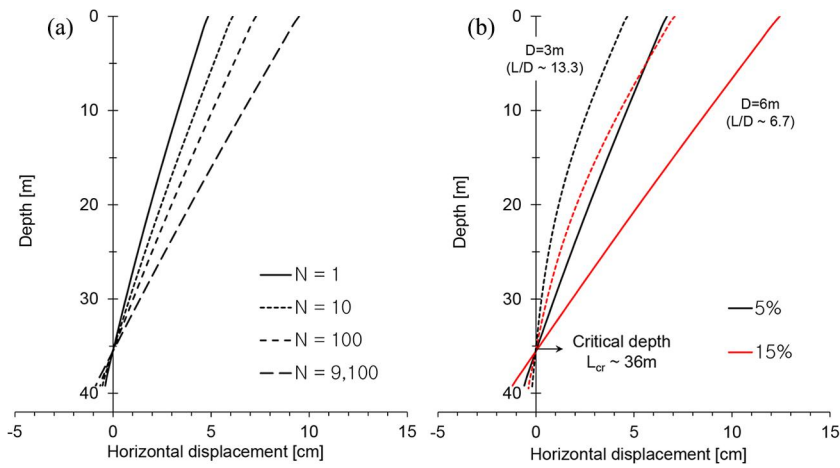
Figure 7 presents the evolution of horizontal displacements along the pile. The pile after the first cycle experiences a displacement transition from compression to extension. In Figure 7a, the critical depth (distance from ground surface to
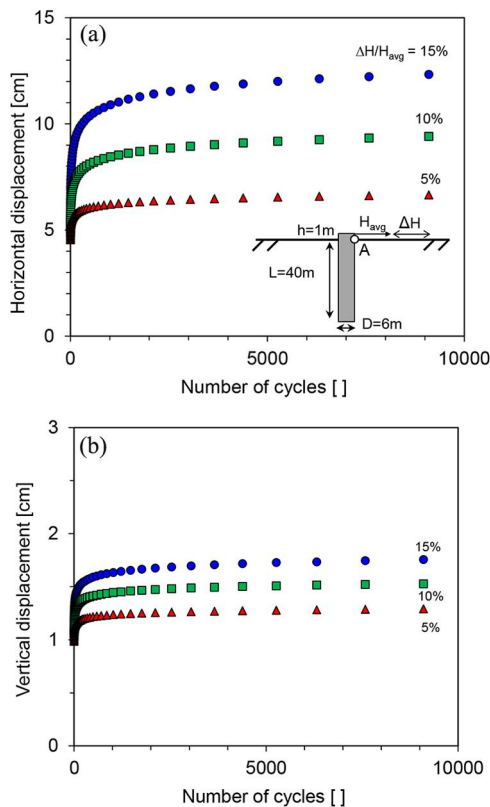
Figure 5. Effect of horizontal load amplitude on the displacement evolution of a pile foundation subjected to repetitive loading: (a) horizontal displacement; (b) vertical displacement. The displacements are measured at the ground surface (point A). The horizontal load amplitudes ΔH are defined by 5, 10, and 15% of average horizontal load $H_{avg} \sim 3.6$ MN (FS $= H_{ult}/H_{avg} \sim 6$).
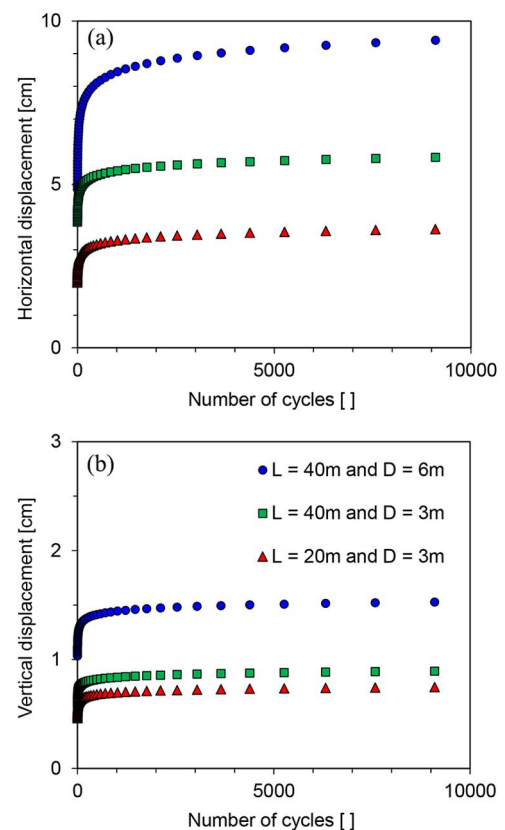
Figure 6. Effect of pile geometries (embedded pile depth L and diameter D) on the displacement evolution of a pile foundation subjected to repetitive loading: (a) horizontal displacement; (b) vertical displacement. The horizontal load amplitude ratio $\Delta H/H_{avg}$ is 10% in all cases.

Figure 7. Evolution of horizontal displacement along a monopile foundation: (a) number of cycles ($D = 6$ m and $\Delta H/H_{avg} = 10\%$); (b) horizontal load amplitudes ($N = 9,100$). The displacements are measured at nodes along the pile.

the transition point) remains constant after the number of cycles while the horizontal displacement gradually evolves from the zero displacement point. Higher horizontal load amplitude increases the displacement along the pile (Figure 7b). The trends of horizontal displacement are significantly affected by the relative pile geometry ratio. A low L/D ratio ($L/D \sim 6.7$) exhibits a rigid pile response where the displacement linearly increases from the embedded pile depth. Meanwhile, a flexible pile ($L/D \sim 13.3$) shows a

nonlinear pattern of displacement where the incremental rate of displacement largely increases toward the ground surface. Note that this study uses the pile geometric ratio to identify pile response; $L/D > 10$ (longer pile embedded length) behaves as flexible pile, otherwise it behaves as a rigid pile (Peng, Clarke, and Rouainia 2011; Arshad and O'Kelly 2016).

The variation in horizontal stress along the pile is explored as shown in Figure 8. The rotation point in both piles moves
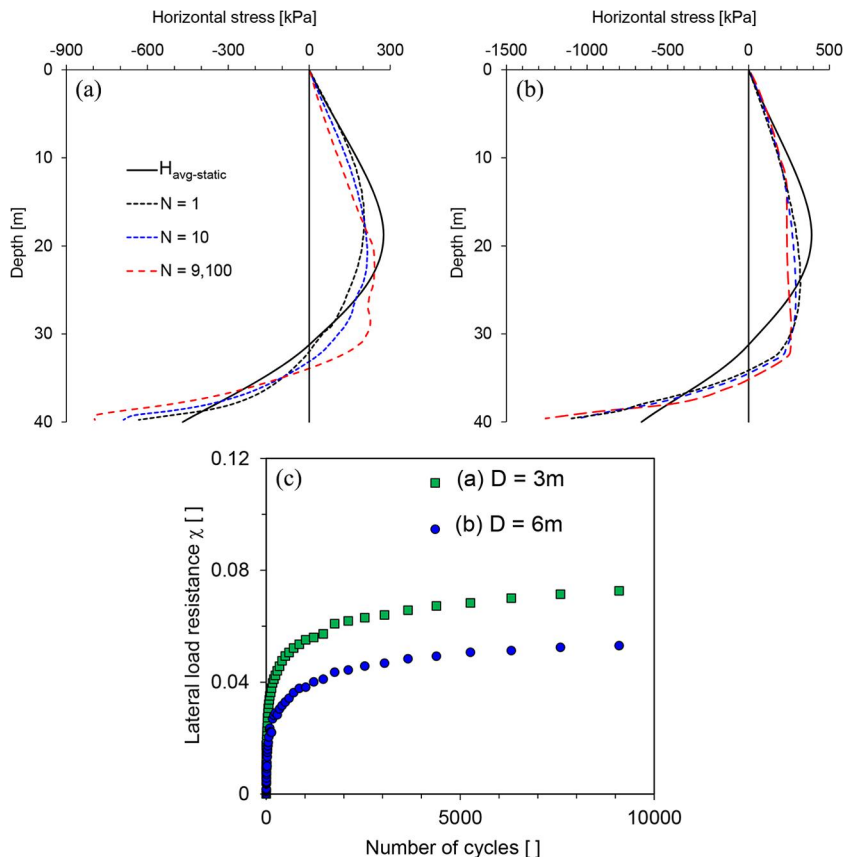
Figure 8. Change in lateral stress along a monopile foundation subjected to repetitive lateral loads: redistribution of lateral stress with (a) $D = 3$ m (flexible pile); (b) $D = 6$ m (rigid pile) for load cycles $N = 1, 100, 9,100$; (c) evolution of lateral load resistance. Continuous line in (a) and (b) is obtained from ultimate lateral resistance (Zhang, Silva, and Grismala 2005) divided by FS = 6.

Table 2. The merits and demerits of the semiempirical scheme that incorporates modified Cam-Clay model into polynomial strain function.

Merits
The explicit scheme helps to avoid larger accumulation of numerical errors compared to physical deformation
Empirical strain function contains the fundamental features for the long-term soil response of geomaterials: volumetric strain (terminal void ratio) and shear strain (shakedown or ratcheting), strain accumulation rate, and stress obliquity
The use of polynomial-type function saves the computational cost by avoiding a cumbersome numerical cutoff criterion
The modified Cam-Clay (MCC) model can capture the stress-dependent soil stiffness and strength
Demerits
The associate flow rule in MCC model cannot capture the peak deviatoric stress that has been commonly observed in normally consolidated clays
Soil around the monopile subjected to numerous cyclic loading undergoes different stress paths, and thus the selection of mobilized friction angle along the monopile involves large uncertainty.

downward for large number of cycles. The initial regime of active pressure decreases and its magnitude increases around pile end, however, the pile rigidity results in the distinct pattern on passive side. The horizontal stress decreases until the upper part of pile, yet it increases from middle part of pile. The rigid pile (larger diameter) shows that local reduction of the horizontal stress takes place around the middle of the pile. The lateral load resistance in each cycle is calculated from numerical integration of net lateral stress by subtracting the active stress from the passive stress. The lateral load resistance is evaluated in terms of dimensionless ratio

$$\chi = \frac{H_{N=i} - H_{N=1}}{H_{N=1}} \qquad (1)$$

Figure 8c shows the evolution of lateral load resistance with the number of cycles. The repetitive lateral load enhances the lateral load resistance due to soil densification along the pile. In fact, the previous experimental investigation into the long-term pile response revealed that the sediment surrounding the pile subjected to cyclic horizontal load undergoes the densification with granular convection related to particle rearrangement and constant sliding (Cuéllar, Baeßler, and Rücker 2009). Thus, we confirm that finite element analysis involved with the fundamental features is capable of simulating the grain migration and soil convection.

Conclusion

This paper analyzes offshore monopile foundation subjected to repetitive loads. Table 2 summarizes the merits and demerits of the semiempirical numerical scheme. The simple and robust numerical scheme used in this paper presents some clear advantages. The semiempirical explicit scheme is used to calibrate under zero-lateral strain boundary condition by relaxing four model parameters. The long-term monopile simulation shows the horizontal repetitive loads accumulate the vertical and horizontal displacements related to pile rotation while the cyclic horizontal load amplitude ΔH is smaller than ultimate lateral load H_{ult}. The most pronounced displacements occur during early cycles ($N < 100$), yet their incremental rate approaches an asymptotic value. The stable deformation state indicates that the soil around monopile foundation undergoes plastic shakedown.

The pile rigidity affects the pattern of horizontal stress and displacement during number of cycles. In particular, the repetitive lateral load enhances the lateral load resistance followed by soil densification along the pile. Thus, the analysis highlights that there is the need to investigate the change of ultimate load induced by long-term movements of the pile. As further study, extensive parametric cases including pile geometry will be simulated and summarized for design practice of offshore foundations.

References

Achmus, M., Y.-S. Kuo, and K. Abdel-Rahman. 2009. Behavior of monopile foundations under cyclic lateral load. *Computers and Geotechnics* 36 (5):725–35. doi:10.1016/j.compgeo.2008.12.003

Arshad, M., and B. C. O'Kelly. 2016. Model studies on monopile behavior under long-term repeated lateral loading. *International Journal of Geomechanics* 17:04016040. doi:10.1061/(asce)gm.1943-5622.0000679

AWS Truewind. 2009. *Offshore wind technology overview*. New York, Long Island: Offshore Wind Collaborative.

Chong, S.-H., and J. C. Santamarina. 2016. Sands subjected to vertical repetitive loading under zero lateral strain: Accumulation models, terminal densities, and settlement. *Canadian Geotechnical Journal* 53 (12):2039–46. doi:10.1139/cgj-2016-0032

Cuéllar, P., M. Baeßler, and W. Rücker. 2009. Ratcheting convective cells of sand grains around offshore piles under cyclic lateral loads. *Granular Matter* 11 (6):379–90. doi:10.1007/s10035-009-0153-3

François, S., C. Karg, W. Haegeman, and G. Degrande. 2010. A numerical model for foundation settlements due to deformation accumulation in granular soils under repeated small amplitude dynamic loading. *International Journal for Numerical and Analytical Methods in Geomechanics* 34 (3):273–96. doi:10.1002/nag.807

Kuo, Y.-S., M. Achmus, and K. Abdel-Rahman. 2012. Minimum embedded length of cyclic horizontally loaded monopiles. *Journal of Geotechnical and Geoenvironmental Engineering* 138 (3):357–63. doi:10.1061/(asce)gt.1943-5606.0000602

Malhotra, S. 2010. Design and construction considerations for Offshore Wind Turbine Foundations in North America. *GeoFlorida* 2010:1533–42. doi:10.1061/41095(365)155

Muir Wood, D. 1990. *Soil behaviour and critical state soil mechanics.* Cambridge University Press, Cambridge, U.K.

Niemunis, A., T. Wichtmann, and T. Triantafyllidis. 2005. A high-cycle accumulation model for sand. *Computers and Geotechnics* 32 (4):245–63. doi:10.1016/j.compgeo.2005.03.002

Pasten, C., H. Shin, and J. Santamarina. 2014. Long-term foundation response to repetitive loading. *Journal of Geotechnical and Geoenvironmental Engineering* 140 (4):04013036. doi:10.1061/(asce)gt.1943-5606.0001052

Peng, J., B. G. Clarke, and M. Rouainia. 2011. Increasing the resistance of piles subject to cyclic lateral loading. *Journal of Geotechnical and Geoenvironmental Engineering* 137 (10):977–82. doi:10.1061/(asce)gt.1943-5606.0000504

Suiker, A. S. J., and R. de Borst. 2003. A numerical model for the cyclic deterioration of railway tracks. *International Journal for Numerical Methods in Engineering* 57 (4):441–70. doi:10.1002/nme.683

Tiwari, B., and A. R. Al-Adhadh. 2014. Influence of relative density on static soil–structure frictional resistance of dry and saturated sand. *Geotechnical and Geological Engineering* 32 (2):411–27. doi:10.1007/s10706-013-9723-6

Wichtmann, T., A. Niemunis, and T. Triantafyllidis. 2005. Strain accumulation in sand due to cyclic loading: Drained triaxial tests. *Soil Dynamics and Earthquake Engineering* 25 (12):967–79. doi:10.1016/j.soildyn.2005.02.022

Zhang, L., F. Silva, and R. Grismala. 2005. Ultimate lateral resistance to piles in cohesionless soils. *Journal of Geotechnical and Geoenvironmental Engineering* 131 (1):78–83. doi:10.1061/(asce)1090-0241(2005)131:1(78)